ionization from the metal d levels, second, ionizations from the β-diketonate ligand, and then, ionization from an olefin orbital.

The differences in electronic structure in these complexes are very well demonstrated in the shifts of the various orbitals. These shifts show that, when a substituent is introduced in a ligand, the electronic effect of this substituent affects the whole molecule. CNDO calculations on model complexes suggest that this is caused by low-lying orbitals which are delocalized over the entire molecule. The trends in the IE's follow the normal electron-withdrawing and -donating properties of the substituents. Shifts in the olefin orbitals can be interpreted in the Chatt–Dewar–Ducanson model as differences in σ and π interactions. π back-bonding especially is of importance in the metal–olefin bond.

The stabilization of the ligand orbitals on going from rhodium to iridium can indicate that σ bonding becomes more important in the iridium complexes.

Registry No. tmhRh$(CO)_2$, 24151-60-8; acacRh$(CO)_2$, 14874-82-9; tfaRh$(CO)_2$, 18517-13-0; tmhRh$(C_2H_4)_2$, 64466-15-5; acacRh$(C_2H_4)_2$, 12082-47-2; tfaRh$(C_2H_4)_2$, 69372-77-6; hfaRh$(C_2H_4)_2$, 55188-59-5; tmhRh$(C_3H_6)_2$, 69372-72-1; acacRh$(C_3H_6)_2$, 12282-38-1; tmhIr$(CO)_2$, 74684-28-9; acacIr$(CO)_2$, 14023-80-4; tfaIr$(CO)_2$, 14024-04-5; hfaIr$(CO)_2$, 14049-69-5; tmhIr$(C_2H_4)_2$, 74684-29-0; acacIr$(C_2H_4)_2$, 52654-27-0; tfaIr$(C_2H_4)_2$, 74684-30-3; acacIr$(C_3H_6)_2$, 66467-05-8; tfaIr$(C_3H_6)_2$, 74684-31-4.

Contribution from the Anorganisch Chemisch Laboratorium, University of Amsterdam, J. H. van't Hoff Instituut, 1018 WV Amsterdam, The Netherlands, and the Departments of Chemistry, The University, Southampton S09 5NH, United Kingdom, and Tulane University, New Orleans, Louisiana 70118

Photochemistry of Piperidine Pentacarbonyl Complexes of the Group 6B Metals Isolated in an Argon Matrix at 10 K

GOSSE BOXHOORN, GERARD C. SCHOEMAKER, DERK J. STUFKENS, AD OSKAM,* ANTHONY J. REST,* and DONALD J. DARENSBOURG*

Received March 26, 1980

Short-wavelength photolysis (λ = 229, 254 nm) of M$(CO)_5$(pip) complexes (pip = piperidine; M = Cr, Mo, W) in Ar matrices at 10 K resulted in the formation of M$(CO)_4$L species with C_s symmetry; long-wavelength photolysis (λ = 366, 405 nm) caused M–L bond breaking and formation of M$(CO)_5$. The structures of the photoproducts were determined by ^{13}CO labeling and force field calculations. The piperidine complexes showed a metal-dependent photochemistry and a reduced photochemical efficiency with respect to other M$(CO)_5$L complexes at all wavelengths. The results are compared with studies of M$(CO)_5$L complexes (M = Cr, W; L = pyridine, pyrazine, NMe_3), both in matrices at 10 K and in solutions at room temperature, and are explained by d-orbital energy diagrams derived from photoelectron spectra.

Introduction

The solution photochemistry of M$(CO)_5$L complexes (M = Cr, Mo, W; L = amine, imine, phosphine) has been extensively studied by several authors.[1-10] These studies demonstrated that the photochemistry of these complexes is dependent on the wavelength of irradiation, the ligand L, and the metal. Two photochemical reactions are possible: eq 1 and 2. The quantum yields of both reactions are dependent

$$M(CO)_5L \xrightarrow[L']{h\nu} M(CO)_5L' + L \quad (1)$$

$$M(CO)_5L \xrightarrow[L']{h\nu'} M(CO)_4LL' + CO \quad (2)$$

on the wavelength; e.g., reaction 1 is dominant at long wavelengths, whereas reaction 2 becomes increasingly important at shorter wavelengths. Zink reported that nitrogen-donor complexes show efficient ligand photosubstitution, with a reduced quantum yield for reaction 2, that phosphorus-donor complexes undergo both reactions with high quantum yields, and that a third class of ligands, e.g., CS, showed low quantum yields for both reactions.[5] These conclusions were based on photolysis with only two wavelengths, namely, 405 and 436 nm. The metal dependence of both photochemical reactions has been demonstrated in a study by Darensbourg et al.[7] An increased quantum yield of CO substitution was found on going from W and Mo to Cr. In the presence of ^{13}CO, exclusively equatorial carbonyl photosubstitution occurred, leading to the suggestion that a C_s intermediate is involved in these photochemical reactions.[7]

In order to prove the structure of the intermediates involved in the photochemical reactions of substituted group 6B hexacarbonyls, we carried out matrix isolation studies.[11-18] Rest proved that bulky ligands can be generated in matrices and found evidence for the formation of W$(CO)_5$ after photolysis

* To whom correspondence should be addressed: A.O., University of Amsterdam; A.J.R., The University, Southampton; D.J.D., Tulane University.

(1) M. Wrighton, G. S. Hammond, and H. B. Gray, *Mol. Photochem.*, **5**, 179 (1973).
(2) M. Wrighton, *Inorg. Chem.*, **13**, 905 (1974).
(3) M. Wrighton, *Chem. Rev.*, **74**, 401 (1974), and references therein.
(4) M. Wrighton, H. B. Abramson, and D. L. Morse, *J. Am. Chem. Soc.*, **98**, 4105 (1976).
(5) R. M. Dahlgren and J. I. Zink, *Inorg. Chem.*, **16**, 3154 (1977).
(6) D. J. Darensbourg and M. A. Murphy, *J. Am. Chem. Soc.*, **100**, 463 (1978).
(7) D. J. Darensbourg and M. A. Murphy, *Inorg. Chem.*, **17**, 884 (1978).
(8) C. C. Frazier and H. Kisch, *Inorg. Chem.*, **17**, 2736 (1978).
(9) R. M. Dahlgren and J. I. Zink, *J. Am. Chem. Soc.*, **101**, 1448 (1979).
(10) R. M. Dahlgren and J. I. Zink, *Inorg. Chem.*, **18**, 597 (1979).
(11) M. Poliakoff, *Inorg. Chem.*, **15**, 2022 (1976).
(12) M. Poliakoff, *Inorg. Chem.*, **15** 2892 (1976).
(13) E. L. Varetti, A. Müller, A. M. English, K. R. Plowman, and I. S. Butler, *Z. Anorg. Allg. Chem.*, **446**, 17 (1978).
(14) (a) A. J. Rest and J. R. Sodeau, *J. Chem. Soc., Chem. Commun.*, 696 (1975); (b) T. M. McHugh, A. J. Rest, and J. R. Sodeau, *J. Chem. Soc., Dalton Trans.*, 184 (1979).
(15) G. Boxhoorn and A. Oskam, *Inorg. Chim. Acta*, **29**, 243 (1978).
(16) G. Boxhoorn, D. J. Stufkens, and A. Oskam, *Inorg. Chim. Acta*, **33**, 215 (1979).
(17) G. Boxhoorn, D. J. Stufkens, and A. Oskam, *J. Chem. Soc., Dalton Trans.*, in press.
(18) G. Boxhoorn, A. Oskam, T. M. McHugh, and A. J. Rest, *Inorg. Chim. Acta*, **44**, L1 (1980).

0020-1669/80/1319-3455$01.00/0

Table I. Infrared Frequencies (cm^{-1}) of $M(CO)_5$(pip) in an Ar Matrix at 10 K

assignt	A_1^2	B_1	E	A_1^1	$\nu(^{13}CO)^b$
$Cr(CO)_5$(pip)	2070.1	1977.2	1937.4,[a] 1924.4	1921.7,[a] 1917.5	1904.2
$Mo(CO)_5$(pip)	2076.7	1979.2	1942.0,[a] 1931.8, 1928.2	1924.9,[a] 1922.1 (sh)	1909.9
$W(CO)_5$(pip)	2075.6	1970.4	1932.8,[a] 1926.8	1924.8,[a] 1917.0	1901.3
intensity[c]	w	w	s[a]	m	w

[a] Most intense band. [b] Most intense band of *cis*-$M(CO)_4(^{13}CO)$(pip). [c] w = weak, m = moderate, s = strong.

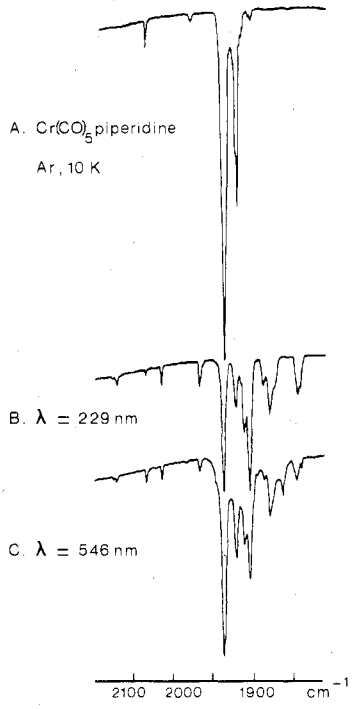

Figure 1. Infrared spectra of $Cr(CO)_5$(pip) in an Ar matrix at 10 K: A, after deposition; B, after 60-min photolysis with λ = 229 nm; C, after further photolysis with λ = 546 nm for 60 min.

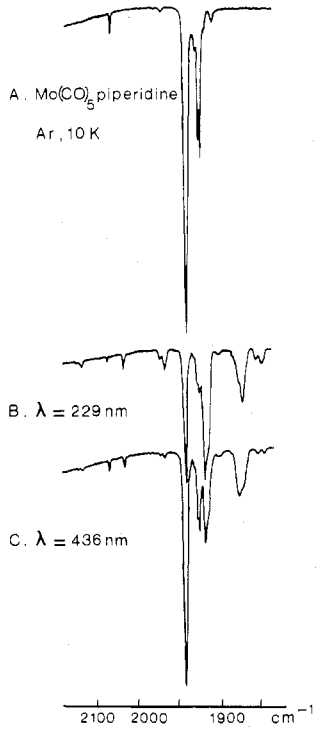

Figure 2. Infrared spectra of $Mo(CO)_5$(pip) in an Ar matrix at 10 K: A, after deposition; B, after 60-min photolysis with λ = 229 nm; C, after further photolysis with λ = 436 nm for 60 min.

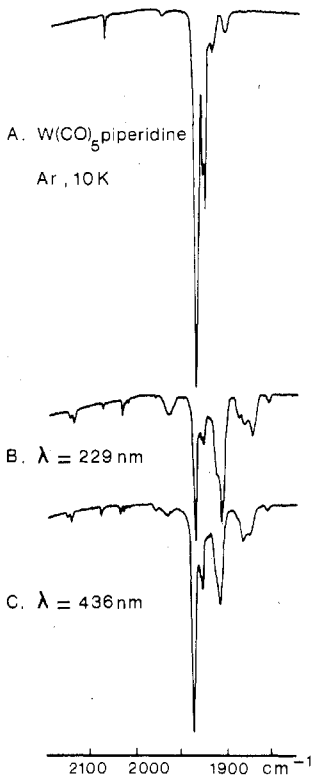

Figure 3. Infrared spectra of $W(CO)_5$(pip) in an Ar matrix at 10 K: A, after deposition; B, after 60-min photolysis with λ = 229 nm; C, after further photolysis with λ = 436 nm for 60 min.

of $W(CO)_5L$ complexes (L = pyridine, 3-bromopyridine, hydrogen sulfide).[14] The same results were observed for $M(CO)_5PCl_3$ complexes (M = Cr, W).[15,16] Photolysis of $M(CO)_5L$ complexes (L = pyridine, pyrazine, NMe_3) yielded both M–L and M–C bond breaking, depending on the wavelength of irradiation.[17,18] All photochemical reactions could be reversed by long-wavelength photolysis.

In this study we describe the photochemical behavior of $M(CO)_5$(pip) complexes (pip = piperidine; M = Cr, Mo, W) in Ar matrices at 10 K. The results are explained with the use of photoelectron and UV–visible spectra. Matrix photochemical reactions are compared with thermochemical data and the results of other photochemical studies in solutions.

Results

IR Spectra. For $M(CO)_5L$ complexes with local C_{4v} symmetry, three CO stretching vibrations are expected (2 A_1 and E). The spectra of the complexes isolated in Ar matrices at 10 K show these three fundamentals, together with several matrix splittings and weak bands between 1970 and 1980 cm^{-1}. These weak bands are assigned to the B_1 modes, which have become allowed by weak distortions of the molecule by the matrix. ^{13}CO satellite bands were detected at about 1905 cm^{-1}. The frequencies of these $M(CO)_5$(pip) complexes closely correspond to previously reported frequencies[10,14,16,17] and are shown in Table I.

UV–Visible Spectra. The electronic absorption spectra of the $M(CO)_5$(pip) complexes show two main bands. One band,

Table II. UV-Visible Absorption Bands (nm) of $M(CO)_5$(pip), $M(CO)_5$, and C_s $M(CO)_4$(pip) in an Ar Matrix at 10 K

assignt	d → π* (CO)	d → d	d → d	d → d (S → T)
$Cr(CO)_5$(pip)	246		414	
$Mo(CO)_5$(pip)	*a*		389	
$W(CO)_5$(pip)	242, 271, 284 (sh)	334, 374	397, 403, 410 (sh)	446
$Cr(CO)_5$	*a*		~530	
$Mo(CO)_5$	*a*		436	
$W(CO)_5$	*a*		442	
C_s $Cr(CO)_4$(pip)	*a*	352	*a*	
C_s $Mo(CO)_4$(pip)	*a*	308	~470	
C_s $W(CO)_4$(pip)	*a*	301	~480	

[a] Not measured.

belonging to a M → π*(CO) transition was detected at about 250 nm. The second band was observed between 380 and 420 nm and was dependent on the central metal atom. This latter band belongs to the spin-allowed $^1E_a(b_2^2e^3a^1) \leftarrow {}^1A_1(b_2^2e^4)$ transition. The assignment of this band has been the subject of some controversy; however, a magnetic circular dichroism (MCD) study of a series of $Cr(CO)_5L$ complexes (L = piperidine, pyridine, pyrazine, NMe_3) proved that this assignment was correct.[19] The corresponding $^3E \leftarrow {}^1A_1$ ligand field transition was only found for the tungsten derivatives. Besides these bands, the UV–visible absorption spectrum of the tungsten complex showed two weak absorptions, which could only be resolved with use of a curve-fitting program.[20] These bands have been attributed either to a third charge transfer transition or to the other possible ligand field transitions: $^1E_b(b_2^2e^3b_1^1) \leftarrow {}^1A_1(b_2^2e^4)$ or $^1A_2(b_2^1e^4b_1^1) \leftarrow {}^1A_1(b_2^2e^4)$. With the aid of MCD we hope to make a definite assignment. In Table II the data of the absorption spectra are compiled.

Photochemistry. Irradiation of $M(CO)_5$(pip) (M = Cr, Mo, W) with wavelengths of 229 and 254 nm resulted in the formation of C_s $M(CO)_4$(pip), for which the structure was proved by ^{13}CO labeling and force field calculations (lower case) (see eq 3). The observed frequencies for the M-

$$M(CO)_5(pip) \underset{\substack{\lambda = 436 \text{ nm for M = Mo,W} \\ \lambda = 546 \text{ nm for M = Cr}}}{\overset{\lambda = 229,\ 254 \text{ nm}}{\rightleftharpoons}} M(CO)_4(pip)\ (C_s) + CO \quad (3)$$

$(CO)_4$(pip) species closely resemble the frequencies found for $Cr(CO)_4L$ (L = pyridine, NMe_3) and $W(CO)_4L$ (L = pyridine).[16-18] Apart from the new bands of C_s $M(CO)_4$(pip), the vibration of free CO was detected at about 2140 cm^{-1}, and weak modes of the pentacarbonyl photoproduct were detected between 1960 and 1970 cm^{-1}. The band between 1960 and 1970 cm^{-1} is the strongest mode (E) of $M(CO)_5$.[21] In the UV–visible absorption spectra the parent bands decreased and new bands appeared between 300 and 360 nm and between 460 and 490 nm (weak). A blue shift of the absorption bands was measured on going from Cr to Mo and W, as was also found for the parent absorption bands (Table II). The reactions were reversed by irradiation into these new absorption bands (e.g., λ = 546 nm for M = Cr and λ = 436 nm for M = Mo, W). Prolonged photolysis yielded lower carbonyl fragments as $M(CO)_3$(pip) (weak bands in the region between 1860 and 1800 cm^{-1}, as is shown in Figures 1–3), together with a complex with bands at 2016.3 (w) and 1881.7 (s), 2022.9 (w) and 1878.9 (s), and 2023.4 (w) and 1880.0 (s) cm^{-1} for

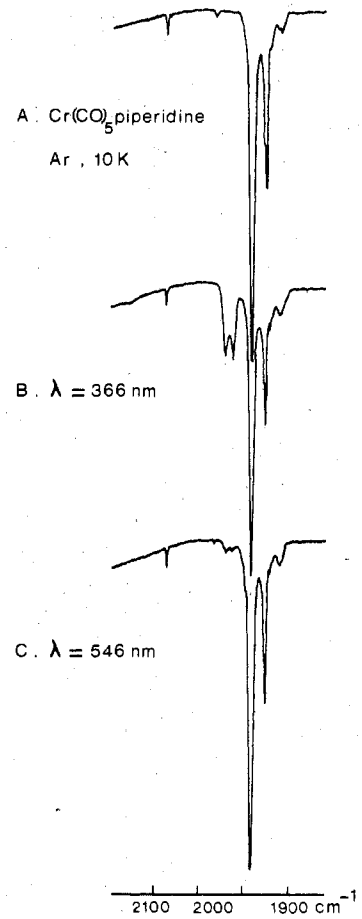

Figure 4. Infrared spectra of $Cr(CO)_5$(pip) in an Ar matrix at 10 K: A, after deposition; B, after 1000-min photolysis with λ = 366 nm; C, after further photolysis with λ = 546 nm for 60 min.

Cr, Mo, and W, respectively. No conclusions could be drawn about the structure of this complex, even after ^{13}CO labeling, since the intensities of the bands were too low.

Enhancement of M–N bond breaking was found upon going to longer wavelength irradiation (see eq 4). Photolysis with

$$M(CO)_5L \underset{\substack{\lambda = 436 \text{ nm for M = Cr} \\ \lambda = 436 \text{ nm for M = Mo,W} \\ \lambda = 546 \text{ nm for M = Cr}}}{\overset{\lambda = 366,\ 405 \text{ nm for M = Cr, Mo, W}}{\rightleftharpoons}} M(CO)_5 + L \quad (4)$$

wavelengths of 366 and 405 nm resulted almost exclusively in formation of $M(CO)_5$ for M = Cr, Mo, and W, as concluded from the new $M(CO)_5$ frequencies at about 1965 cm^{-1}. For M = Cr, pentacarbonyl formation was also detected with λ = 436 nm. The reaction was reversed after irradiation into the absorption bands of the pentacarbonyls. The infrared and UV–visible spectra, before and after photolysis, are shown in Figures 1–8. The frequencies of the photolysis products are compiled in Table III.

^{13}CO Labeling and Force Field Calculations. $M(CO)_5$(pip). For the assignment of the infrared frequencies of the isomers we used force field calculations. Initial force constants were chosen from the labeling experiments with $Cr(CO)_5NMe_3$.[17] This set of force constants was refined with the aid of the observed wavenumbers of the isomers and an iterative computer program. We used a force field of the CO-stretching region without any interaction with other vibrations. Most bands were calculated within one wavenumber. The wavenumbers of these bands and the refined force constants are tabulated in Table IV.

$M(CO)_4$(pip). Photolysis with λ = 229 and 254 nm of the labeled $M(CO)_5$(pip) complexes in Ar at 10 K resulted in the

(19) G. Boxhoorn, D. J. Stufkens, P. J. F. M. v. d. Coolwijk, and A. M. F. Hezemans, *J. Chem. Soc., Chem. Commun.*, 1075 (1979); submitted for publication in *Inorg. Chem.*

(20) D. A. Wensky and A. K. Wensky, *Spectrochim. Acta, Part A*, **31A**, 23 (1975).

(21) H. Daamen and A. Oskam, *Inorg. Chim. Acta*, **26**, 81 (1978), and references therein.

Table III. Infrared Frequencies (cm^{-1}) of the Photolysis Products of $M(CO)_5(pip)$ in Ar at 10 K

assignt	A_1	A′	E	A_1	A′	A″
$Cr(CO)_5$	*a*		1964.7, 1956.3	*b*		
$Mo(CO)_5$	*a*		1972.9, 1967.3 (sh)	*b*		
$W(CO)_5$	*a*		1964.0, 1958.0 (sh)	*b*		
C_s $Cr(CO)_4(pip)$		2031.2			1912.4, 1905.7	1888.9, 1881.7
C_s $Mo(CO)_4(pip)$		2039.7			1924.6, 1919.6, 1914.5 (sh)	1873.5
C_s $W(CO)_4(pip)$		2035.9			1909.8, 1904.0	1886.4, 1871.5

[a] Band too weak to observe under experimental conditions of relatively small amounts of sample on the window and relatively low photochemical conversion. [b] Band obscured by bands of $M(CO)_5(pip)$.

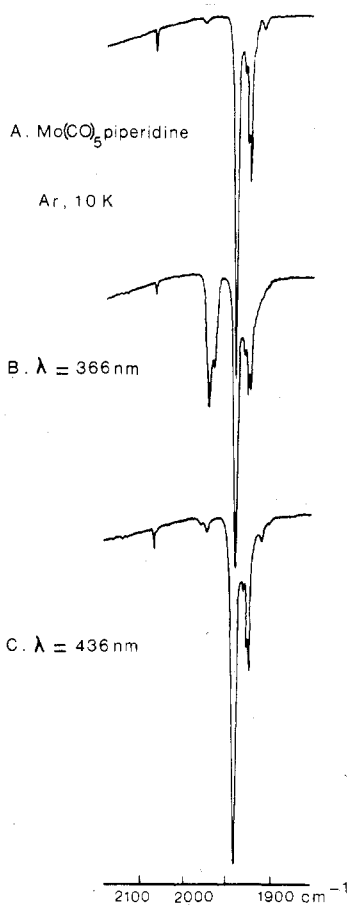

Figure 5. Infrared spectra of $Mo(CO)_5(pip)$ in an Ar matrix at 10 K: A, after deposition; B, after 1000-min photolysis with $\lambda = 366$ nm; C, after further photolysis with $\lambda = 436$ nm for 60 min.

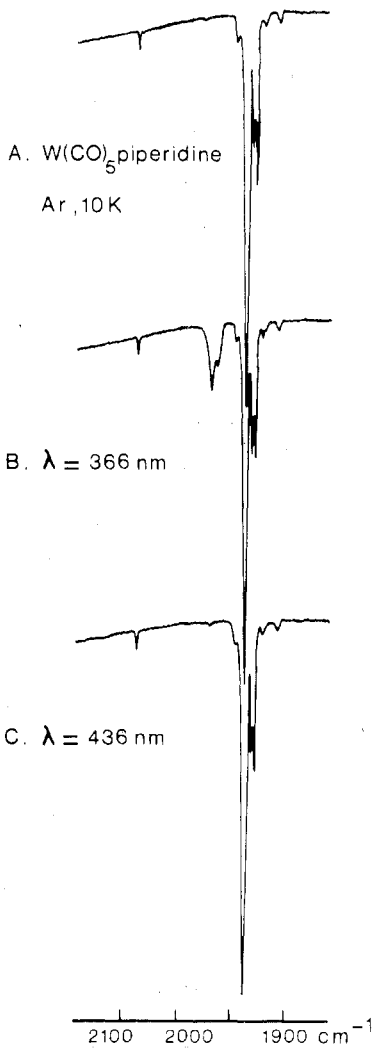

Figure 6. Infrared spectra of $W(CO)_5(pip)$ in an Ar matrix at 10 K: A, after deposition; B, after 1000-min photolysis with $\lambda = 366$ nm; C, after further photolysis with $\lambda = 436$ nm for 60 min.

formation of labeled $M(CO)_4(pip)$ species. From the number and intensity of the bands we assumed that the symmetry of the $M(CO)_4(pip)$ photolysis product could only be C_s, in agreement with $Cr(CO)_4NMe_3$.[17] The initial set of force constants was chosen from the experiments with labeled $Cr(CO)_4NMe_3$. The refinement of the force constants with the aid of all observed frequencies gave the final set of force constants. The calculated frequencies are compiled in Table V, and the agreement with the observed frequencies leads to the conclusion that the assumption of C_s symmetry was right.

Discussion

For the explanation of the photochemical behavior of group 6B substituted carbonyl complexes we make use of a d-orbital energy diagram (Figure 9). Photoelectron measurements give information about the occupied molecular orbitals, while the position and character of the lowest unoccupied molecular orbital can be derived from the UV–visible and MCD spectra. Previous results[16] have shown that population of the σ-antibonding d_{z^2} orbital by long-wavelength irradiation results in almost exclusive formation of $M(CO)_5$, whereas population of the σ-antibonding $d_{x^2-y^2}$ orbital causes the labilization of the M–C bonds of the equatorial CO groups. This labilization

Table IV. Observed (Calculated) Frequencies (cm^{-1}) of $M(CO)_4(^{13}CO)(pip)$ in an Ar Matrix at 10 K

$Cr(CO)_5(pip)$	2070.1	1977.2	1937.4	1937.4	1921.7
	(2070.6)	(1977.0)	(1936.9)	(1936.9)	(1921.0)
eq $Cr(CO)_4$-	2063.0	1970.2	1937.4[a]	1921.7	1905.0
$(^{13}CO)(pip)$	(2062.5)	(1970.0)	(1937.0)	(1922.2)	(1906.7)
$W(CO)_5(pip)$	2075.6	1970.4	1932.8	1932.8	1924.8
	(2076.2)	(1971.2)	(1932.7)	(1932.7)	(1924.6)
eq $W(CO)_4$-	2068.6	1965.4	1932.8[a]	1924.8[a]	1902.4
$(^{13}CO)(pip)$	(2068.0)	(1964.4)	(1932.7)	(1925.0)	(1903.0)

[a] Coinciding bands. The refined force constants are as follows: for M = Cr, $k_1 = 1580.2$, $k_5 = 1510.4$, $k_{12} = 33.3$, $k_{15} = 33.2$, and $k_{13} = 65.0$ N m^{-1}; for M = W, $k_1 = 1575.7$, $k_5 = 1520.4$, $k_{12} = 36.8$, $k_{15} = 36.7$, and $k_{13} = 67.3$ N m^{-1}.

Table V. Observed (Calculated) Frequencies (cm^{-1}) of $M(CO)_3(^{13}CO)(pip)$ in an Ar Matrix at 10 K

C_s $Cr(CO)_4(pip)$	2031.2 (2030.9)	1912.4 (1912.6)	1905.7 (1905.7)	1888.9 (1889.3)
C_1 (fac)$Cr(CO)_3$-$(^{13}CO)(pip)$	2018.9 (2019.3)	*a* (1911.0)	1888.9 (1889.3)	1875.4 (1875.5)
C_s (mer)$Cr(CO)_3$-$(^{13}CO)(pip)$	*a* (2024.5)	*a* (1907.1)	1905.7[b] (1905.7)	1859.4 (1858.3)
C_s $W(CO)_4(pip)$	2035.9 (2035.5)	1909.8 (1909.4)	1904.0 (1903.4)	1886.4 (1885.8)
C_1 (fac)$W(CO)_3$-$(^{13}CO)(pip)$	2023.4 (2023.9)	*a* (1908.0)	1886.4[b] (1885.9)	1871.4 (1873.0)
C_s (mer)$W(CO)_3$-$(^{13}CO)(pip)$	*a* (2028.8)	*a* (1903.9)	1904.0[b] (1903.4)	1853.6 (1855.1)

[a] Not detected. [b] Coinciding bands. The refined force constants are as follows: for M = Cr, $k_2 = 1532.7$, $k_3 = 1492.0$, $k_5 = 1494.2$, $k_{23} = 45.9$, $k_{24} = 65.8$, $k_{25} = 44.5$, and $k_{35} = 51.4$ N m^{-1}; for M = W, $k_2 = 1531.7$, $k_3 = 1489.9$, $k_5 = 1492.1$, $k_{23} = 49.1$, $k_{24} = 68.3$, $k_{25} = 47.7$, and $k_{35} = 54.6$ N m^{-1}.

of the M–C bonds is accomplished by short-wavelength irradiation (λ = 229 and 254 nm). The energy difference ΔE between these two σ^* orbitals can be estimated from photoelectron[21] and UV–visible data (see Figure 9). This energy difference is dependent on the metal and the ligand. The order for ΔE is $Cr(CO)_5NMe_3 > Cr(CO)_5(pip) \approx W(CO)_5(pip) > Cr(CO)_5(py) > Cr(CO)_5(pyr)$ (pyr = pyrazine) > $W(CO)_5(py)$. Unfortunately photoelectron measurements of $Mo(CO)_5(pip)$ failed, because of rapid thermal disproportionation into $Mo(CO)_6$. It is expected that ΔE will strongly influence the photochemical behavior, since a large energy difference will reduce the rate of internal conversion between the b_1 ($d_{x^2-y^2}$) and a_1 (d_{z^2}) orbitals, leading to lower yields of $M(CO)_5$ after short-wavelength irradiation. Besides ΔE, other effects can influence the photochemical behavior, as will be discussed below. In Table VI, the relation between ΔE and the observed matrix photochemical behavior (deduced from infrared intensities as described in Table VI) is seen. The photochemical behavior expected from photoelectron and UV–visible data agrees very well with the observed yields of matrix photoproducts, although there are some differences.

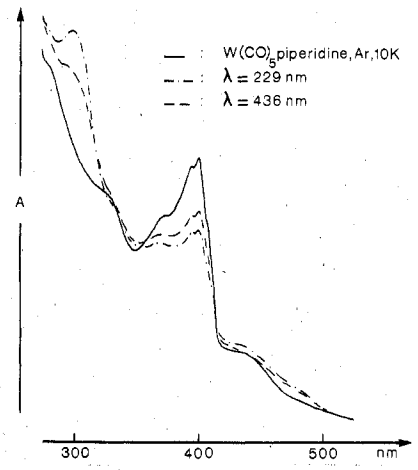

Figure 7. UV–Visible absorption spectra of $W(CO)_5(pip)$ in an Ar matrix at 10 K: —, after deposition; –·–, after 90-min photolysis with λ = 229 nm; – –, after 60-min photolysis with λ = 436 nm.

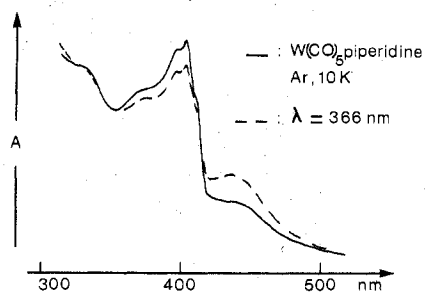

Figure 8. UV–Visible absorption spectra of $W(CO)_5(pip)$ in an Ar matrix at 10 K: —, after deposition; – –, after 1020 min photolysis with λ = 366 nm.

Irradiation with λ = 366 nm increases the formation of $Mo(CO)_5$, and this is probably caused by the blue shift of the $^1E \leftarrow {}^1A_1$ transition upon going from Cr and W to Mo. This fact also explains the higher yields of $Cr(CO)_5$ at the wavelengths 405 and 436 nm. However, if photolysis of $M(CO)_5(pip)$ (M

Table VI. Relation between the Photochemical Reactivity in Matrices at 10 K and in Solutions at Room Temperature and the Expected Yield Based on ΔE and on the Nitrogen Bond Enthalpy, Respectively

Formation of $M(CO)_5$

			expected yield	
λ, nm	reactivity in matrices[h]	quantum yield solns	based on ΔE	based on the nitrogen bond enthalpy
229	Cr(pip) ≈ Mo(pip) ≈ W(pip)[a,b] W(py) > W(pip) W(py) > Cr(py) Cr(pyr) ≈ Cr(py) > Cr(pip) > CrN	no data available		
313	Mo(pip) > Cr(pip) ≈ W(pip)	W(pip) > Mo(pip) > Cr(pip)	Cr(pip) ≈ W(pip)[e]	Cr(pip) > Mo(pip) > W(pip)
334	Mo(pip) > Cr(pip) ≈ W(pip)	no data available	W(py) > W(pip)	W(py) > W(pip)
366	Mo(pip) > Cr(pip) ≈ W(pip) Cr(pyr) > Cr(py) > CrN > Cr(pip)	Mo(pip) > W(pip) > Cr(pip) Cr(pip) > Cr(py)	W(py) > Cr(py) Cr(pyr) > Cr(py) > Cr(pip) > CrN	Cr(py) > W(py) Cr(pyr) > Cr(py) > Cr(pip)[f]
405	Cr(pip) > Mo(pip) > W(pip) CrN > Cr(pyr) ≈ Cr(py) > Cr(pip)	no data available[d]		
436	Cr(pip) > Mo(pip) = W(pip)[c] CrN > Cr(pyr) ≈ Cr(py) > Cr(pip)	no data available[d]		

Formation of C_s $M(CO)_4L$

λ, nm	reactivity in matrices	quantum yield solns	λ, nm	reactivity in matrices	quantum yield solns
229	Cr(pip) ≈ Mo(pip) > W(pip)[g] CrN > Cr(pyr) ≈ Cr(py) ≈ Cr(pip)	no data available	313	Cr(pip) > Mo(pip) > W(pip)	Cr(pip) > Mo(pip) > W(pip) Cr(pip) > Cr(py)
			334	Cr(pip) > Mo(pip) > W(pip)	no data available

[a] Only small yields. [b] pip = piperidine, pyr = pyrazine, py = pyridine, and N = NMe_3. [c] No formation of $M(CO)_5$ was detected for M = Mo and W. [d] Only $W(CO)_5(pip)$ and $W(CO)_5(py)$ were measured. [e] Attempts to measure PES of $Mo(CO)_5(pip)$ failed. [f] No data available for $Cr(CO)_5NMe_3$. [g] Small differences. [h] It has to be noted, that the reactivities in matrices were determined by measuring infrared intensities of product bands. If we correct for differences in extinctions at the various wavelengths, the differences between matrices and solutions remain. In solutions, however, quantum yields have been calculated.

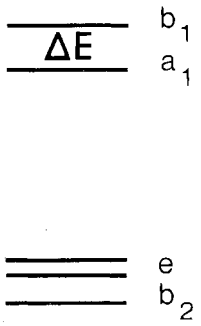

Figure 9. d-Orbital energy diagram of $M(CO)_5L$ complexes.

= Mo, W) with λ = 436 nm leads to M–L bond breaking, this reaction would be reversed, since the visible absorption bands of $M(CO)_5$ (M = Mo, W) lie in this region. These results show that general conclusions about photochemical behavior can only be drawn after irradiation within all absorption bands.

Going from pyrazine, pyridine, and piperidine to NMe_3, a red shift is detected in the absorption spectra for the lowest ligand field transition. This shift is, however, very small and cannot fully explain the higher yield of $Cr(CO)_5$ after irradiation of $Cr(CO)_5NMe_3$ with the wavelengths 405 and 436 nm. These differences are probably caused by the differences in "bulkiness" and steric hindrance of the ligand. From thermochemical measurements we can estimate the nitrogen bond enthalpy, and these figures give information about the M–N bond strength[22] and hence give an indication of the expected yields of $M(CO)_5$. The conclusions (see Table VI) are in good agreement with the observed photochemical behavior, although there is one anomaly: we detected a relative M–N bond breaking order: $W(CO)_5(py) > Cr(CO)_5(py)$. An explanation for this effect can be that, although the M–N bond in $W(CO)_5(py)$ is stronger than in $Cr(CO)_5(py)$, the spin–orbit coupling decreases together with an increase of ΔE in going from W to Cr and that these effects are stronger than the bonding effect.

High-energy irradiation resulted in the formation of $M(CO)_4L$, and this photochemical reaction was influenced both by the central metal atom and by the ligand. Going from Cr and Mo to W, a decrease of $M(CO)_4(pip)$ formation was detected, and this is explained by the increase of spin–orbit coupling, leading to deactivation of the excited states. It should be noted that $W(CO)_5L$ complexes show luminescence at low temperatures, whereas some $Mo(CO)_5L$ complexes luminescence weakly and $Cr(CO)_5L$ complexes rarely luminesce.[23] At this moment we cannot explain the ligand influence on the photochemical behavior at short wavelengths, although high-frequency ligand modes are able to deactivate excited states.[24,25]

Solution Photochemistry and Matrix Isolation Photochemistry. The photochemistry of transition-metal piperidine complexes in matrices at low temperatures differs somewhat from the photochemistry in solutions at room temperature (Table VI).[7] This phenomenon was also observed in the studies of $M(CO)_5CS$[11,12] and $M(CO)_5PCl_3$,[15,16] where in matrices only CO rupture was detected for $M(CO)_5CS$, but in solution both possible reactions were observed with low quantum efficiency.[5] For $M(CO)_5PCl_3$ only M–P bond breaking was accomplished in matrices in contrast to solutions where both reactions took place, with reduced quantum efficiency for the formation of $M(CO)_6$. The reason for these differences is not yet clear. However in solution other factors can mask the nature of the photochemical reaction, e.g., reactions with solvent impurities, thermal decomposition, influences of the solvent, and interactions between the solvent and the photochemical reaction intermediates.

Work is in progress to investigate the details of photophysical processes in low-temperature matrices. For example, luminescence spectra have recently been obtained for $M(CO)_6$ (M = Cr, Mo, W) and $M(CO)_5L$ (M = Mo, W) complexes in gas matrices for the first time.[23] Poliakoff[26] has measured the relative quantum yields for the forward and reverse reactions in eq 5, and we have developed the capability of

$$Mo(CO)_6 \underset{h\nu'}{\overset{h\nu}{\rightleftharpoons}} Mo(CO)_5 + CO \qquad (5)$$

Ar, CH_4, CO; 10 K

measuring luminescence lifetimes down to a few nanoseconds for matrix-isolated molecules.[27] It is anticipated that extensions of such studies will lead to a more detailed understanding of photochemistry in matrices, as well as establish whether the matrix isolation experiment is a good model for proving the primary photoreactions of complexes in solution.

Conclusions

The group 6B metal piperidine complexes showed reduced yields for both photochemical reactions 1 and 2 in comparison with other $M(CO)_5L$ complexes.

Reduced yields for both the formation of $M(CO)_5$ and C_s $M(CO)_4(pip)$ were found for the tungsten complex.

Photochemical behavior is strongly dependent on the wavelength of irradiation, and general conclusions cannot be drawn except after irradiating into all absorption bands.

Matrix isolation photochemistry at 10 K shows some differences with solution photochemistry at room temperature and is better explained by photoelectron, UV–visible, and thermochemical data.

Experimental Section

$M(CO)_5$(pip). The preparation of the $M(CO)_5$(pip) complexes (M = Cr, Mo, W) has been published elsewhere.[7,22]

C_s $Cr(CO)_4(^{13}CO)$(pip). C_{2v} $Cr(CO)_4(pip)_2$ was prepared from $Cr(CO)_6$ and excess piperidine in refluxing heptane. A solid sample of C_{2v} $Cr(CO)_4(pip)_2$ was placed in the side arm of an Schlenkware flask which was fitted with a septum cap and evacuated. Dichloromethane was added to the flask, and the flask was pressurized with carbon monoxide (93.4% ^{13}C) to ~1.2 atm. The flask was tilted to introduce the C_{2v} $Cr(CO)_4(pip)_2$ sample to the ^{13}CO-saturated CH_2Cl_2 solution, and the reaction mixture was stirred at 30 °C for ~1 h. Volatiles were removed under vacuum, and the bright yellow product was recrystallized from hexane at dry-ice temperature.[28] The infrared spectrum of the C_s $Cr(CO)_4(^{13}CO)(pip)$ product showed bands in the $\nu(CO)$ region at 2058, 1968, 1936, 1921, 1905, and 1894 (sh) cm^{-1} (all due to the equatorially ^{13}CO-labeled species). Peak positions are accurate to ±1.0 cm^{-1}. A band at 1878 cm^{-1} was seen, at very high concentration, which is attributed to the presence of C_{4v} $Cr(CO)_4(^{13}CO)(pip)$. That the ^{13}CO incorporation was completely stereoselective was further verified by ^{13}C NMR. The ^{13}C NMR spectrum of $Cr(CO)_4(^{13}CO)(pip)$ revealed the presence of only one carbonyl carbon resonance at 214.2 ppm, whereas a natural-abundance sample of $Cr(CO)_5(pip)$ displays two peaks at 214.2 ($\delta(C_{cis})$) and 220.1 ppm ($\delta(C_{trans})$). C_s $M(CO)_4(^{13}CO)(pip)$ was prepared in a manner analogous to that for the chromium complex. Labeled $Mo(CO)_5(pip)$ could not be used for matrix isolation spectroscopy, as a result of the lower stability of the Mo complex.

Intramolecular Rearrangement of C_s $Cr(CO)_4(^{13}CO)$(pip). Since intramolecular rearrangements in other group 6B carbonyl derivatives have recently been noted to occur by means of a non-bond-breaking

(22) H. Daamen, H. van der Poel, D. J. Stufkens, and A. Oskam, *Thermochim. Acta*, **34**, 69 (1979).
(23) T. M. McHugh, R. Narayanaswamy, A. J. Rest, and K. Salisbury, *J. Chem. Soc., Chem. Commun.*, 208 (1979).
(24) D. J. Robbins and A. J. Thomson, *Mol. Phys.*, **25**, 1103 (1973).
(25) W. Strek and C. J. Ballhausen, *Mol. Phys.*, **36**, 1321 (1978).
(26) M. Poliakoff, *J. Chem. Soc., Faraday Trans. 2*, 73, 569 (1977).
(27) E. P. Gibson, R. Narayanaswamy, A. J. Rest, and K. Salisbury, *J. Chem. Soc., Chem. Commun.*, 925 (1979).
(28) D. J. Darensbourg and R. L. Kump, *J. Organomet. Chem.*, **140**, C29 (1977).

mechanism, it was important to examine the thus formed C_s Cr(CO)$_4$(^{13}CO)(pip) for possible CO scrambling processes.[29-31] C_s Cr(CO)$_4$(^{13}CO)(pip) was sublimed at 52 °C under vacuum to yield a yellow crystalline material. Subjection of this sublimed sample to IR and ^{13}C NMR analysis (vide supra) illustrated that the species maintained the integrity of its CO ligands; i.e., *no* rearrangement of CO ligands was observed.

Equipment. In previous papers, the equipment used to achieve cryogenic temperatures was described, together with photolysis sources and spectrometers.[15-17] The samples were evaporated by using an oven and the slow spray-on method. The evaporation time varied between 45 and 90 min. The oven temperatures for the Cr, Mo, and W complexes were 0–5 °C, room temperature, and 40–50 °C, respectively. The Mo(CO)$_5$(pip) complex was very sensitive to collisions with the glass wall, and decomposition into Mo(CO)$_6$ was detected to be a function of the glass surface. During decomposition the temperature of the NaCl window never exceeded 10 K and the vacuum was better than 10^{-6} torr. Argon with a purity of 99.9997% was employed and sprayed on through a needle valve.

Registry No. Cr(CO)$_5$(pip), 15710-39-1; Mo(CO)$_5$(pip), 19456-57-6; W(CO)$_5$(pip), 31082-68-5; C_s Cr(CO)$_4$(pip), 74764-03-7; C_s Mo(CO)$_4$(pip), 74764-04-8; C_s W(CO)$_4$(pip), 74764-05-9; C_s Cr(CO)$_4$(^{13}CO)(pip), 65255-66-5; C_s W(CO)$_4$(^{13}CO)(pip), 65255-68-7; C_1 *fac*-Cr(CO)$_3$(^{13}CO)(pip), 74764-06-0; C_s *mer*-Cr(CO)$_3$(^{13}CO)(pip), 74806-96-5; C_1 *fac*-W(CO)$_3$(^{13}CO)(pip), 74764-07-1; C_s *mer*-W(CO)$_3$(^{13}CO)(pip), 74806-97-6; C_{2v} Cr(CO)$_4$(pip)$_2$, 65255-70-1; C_{4v} Cr(CO)$_4$(^{13}CO)(pip), 65620-49-7; Cr(CO)$_5$, 26319-33-5; Mo(CO)$_5$, 32312-17-7; W(CO)$_5$, 30395-19-8.

(29) D. J. Darensbourg, *Inorg. Chem.*, **18**, 14 (1979).
(30) D. J. Darensbourg and B. J. Baldwin, *J. Am. Chem. Soc.*, **101**, 6447 (1979).
(31) D. J. Darensbourg, B. J. Baldwin, and J. A. Froelich, *J. Am. Chem. Soc.*, **102**, 4688 (1980).

Contribution from Olson Laboratories of Rutgers—State University, Newark, New Jersey 07102, and Allied Chemical Corporation, Morristown, New Jersey 07960

Photoinduced Electron Transfer from the Cerous Ion Excited State to Cupric Ion

R. P. ASBURY, G. S. HAMMOND,[1a] P. H. P. LEE,[1b] and A. T. POULOS*[1b]

Received March 26, 1980

Photoinduced electron transfer between Ce^{3+}(aq) and Cu^{2+}(aq) in sulfate solution has been studied by microsecond-flash excitation techniques. The photoproducts are cerium(IV) sulfate complexes and Cu^+, which rapidly undergo reverse electron transfer which can be monitored by kinetic spectrophotometry. The rate constant of this thermal reaction ($k = 1.25 \times 10^6$ M^{-1} s^{-1} at 25 °C in 1.0 M acetonitrile) can be slowed by greater than 2 orders of magnitude by varying the solvent from water to 3 M aqueous acetonitrile. There is evidence that the primary photochemical act is bimolecular collision of the lowest energy 4d → 5f excited state of cerous ion with cupric ion. Both fluorescence quantum yields and lifetimes can be correlated with cupric ion concentration and fit Stern–Volmer kinetics. Rate constants for dynamic quenching of Ce^{3+} emission by Cu^{2+}(aq), Fe^{3+}(aq), Cr^{3+}(aq), Tl^{3+}(aq), and Eu^{3+}(aq) are also reported.

Introduction

Ultraviolet excitation of 4f → 5d electronic transitions[2] of Ce^{3+}(aq) in aqueous solution initiates photopolymerization of vinyl compounds and nitriles[3] and causes electron transfer to the hydronium ion[4] and the persulfate anion.[5] The products result from a primary photochemical event followed by thermal reactions; consequently, it is difficult to determine primary-process quantum yields and to study changes in reaction medium on the primary process. To extend understanding of Ce^{3+}(aq) excited-state behavior, yet avoid complications by secondary reactions, we undertook a search for reversible, photoinduced, one-electron-transfer reactions of the type

$$Ce^{3+}(aq) + A^{n+}(aq) \underset{\Delta}{\overset{h\nu}{\rightleftharpoons}} Ce(IV) + A^{(n-1)+}(aq) \quad (1)$$

Incidentally, such reactions *in principle* can generate photogalvanic current.[6] The acceptors, A^{n+}, were chosen by the following criteria: (1) lack of thermal reactivity with Ce^{3+}(aq) or Ce(IV), (2) existence of a stable lower oxidation state, (3) lack of strong ultraviolet absorption in the region of some of the cerous 4f → 5d bands, and (4) low probability of forming ground-state complexes with Ce^{3+}(aq).

We report that electron transfer from excited Ce^{3+}(aq) can be observed spectroscopically with Cu^{2+}(aq) but not with Fe^{3+}(aq), Cr^{3+}(aq), or Eu^{3+}(aq), even though the latter ions efficiently quench Ce^{3+} emission. Studies on the mechanism of the reaction with Cu^{2+} are reported here.

Experimental Section

Reagents. All materials were reagent grade and used without further purification, except for $Ce_2(SO_4)_3$ (Alfa Products), which was recrystallized from water by adding concentrated sulfuric acid to a saturated solution of the salt and allowing the mixture to stand overnight. The concentration of Ce(III) aqueous solutions used for flash excitation or emission quenching was determined by weight or was determined spectrophotometrically from the 4f → 5d band extinction coefficients.[7] $Eu(ClO_4)_3$ (Alfa) and $Cu(SO_4)_2 \cdot 5H_2O$ (Mallinckrodt) concentrations were determined by weight of dry samples. Cr(III) concentrations of $Cr(ClO_4)_3$ (Alfa) solutions were determined by spectrophotometric analysis of the ethylenediaminetetraacetate complex.[8] Fe(III) in solutions of ferric sulfate was determined by weight and from the extinction coefficient (2.175×10^3 M^{-1} cm^{-1} at 305 nm) in 0.8 N H_2SO_4.[9] Tl(III) concentrations were determined by weight of the dry perchlorate salt.

Flash Photolysis. The conventional flash photolysis apparatus was constructed at the University of California—Santa Cruz. The flash tube (Xenon Corp. N-108C) and a 15 × 1 cm^2 sample cell (Pyrex or quartz) were held at the focal points of an elliptical aluminum cavity by ebonite brackets. Up to 100 J of excitation energy (20-μs duration) could be supplied by a Xenon Corp. Model 457A Micropulser. The

(1) (a) Allied Chemical Corp. (b) Rutgers University.
(2) C. K. Jørgensen and J. S. Brinen, *Mol. Phys.*, **6**, 629 (1963).
(3) (a) F. H. C. Edgecombe and R. G. W. Norrish, *Nature (London)*, **197**, 282 (1963). (b) F. Hussain and R. G. W. Norrish, *Proc. R. Soc. London, Ser. A*, **275**, 161 (1963).
(4) L. J. Heidt and A. F. McMillan, *J. Am. Chem. Soc.*, **76**, 2135 (1954).
(5) R. W. Matthews and T. J. Sworski, *J. Phys. Chem.*, **79**, 681 (1975).
(6) M. S. Wrighton, *Chem. Eng. News*, **57**, 29 (1979).
(7) H. L. Greenhans, A. M. Feibush, and Louis Gordon, *Anal. Chem.*, **29**, 1531 (1957).
(8) R. E. Hamm, *J. Am. Chem. Soc.*, **75**, 5670 (1953).
(9) J. Jortner and G. Stein, *J. Phys. Chem.*, **66**, 1258 (1962).

0020-1669/80/1319-3461$01.00/0